Inorg. Chem. **2003**, *42*, 6241–6251

Sterically Encumbered Diphosphaalkenes and a Bis(diphosphene) as Potential Multiredox-Active Molecular Switches: EPR and DFT Investigations

Cosmina Dutan,[†] Shashin Shah,[‡] Rhett C. Smith,[‡] Sylvie Choua,[†] Théo Berclaz,[†] Michel Geoffroy,*[,†] and John D. Protasiewicz*[,‡]

Department of Physical Chemistry, University of Geneva, 30 Quai E. Ansermet, 1211 Geneva 4, Switzerland, and Department of Chemistry, Case Western Reserve University, Cleveland, Ohio 44106-7708

Received February 28, 2003

The reduction products of two diphosphaalkenes (**1** and **2**) and a bis(diphosphene) (**3**) containing sterically encumbered ligands and corresponding to the general formulas Ar–X═Y–Ar′–Y═X–Ar, have been investigated by EPR spectroscopy. Due to steric constraints in these molecules, at least one of the dihedral angles between the CXYC plane and either the Ar plane or the Ar′ plane is largely nonzero and, hence, discourages conformations that are optimal for maximal conjugation of P═X (or P═Y) and aromatic π systems. Comparison of the experimental hyperfine couplings with those calculated by DFT on model systems containing no cumbersome substituents bound to the aromatic rings shows that addition of an electron to the nonplanar neutral systems causes the X═Y–Ar′–Y═X moiety to become planar. In contrast to **1** and **2**, **3** can be reduced to relatively stable dianion. Surprisingly the two-electron reduction product of **3** is paramagnetic. Interpretation of its EPR spectra, in the light of DFT calculations on model dianions, shows that in [**3**]$^{2-}$ the plane of the Ar′ ring is perpendicular to the CXYC planes. Due to interplay between steric and electronic preferences, the Ar–X═Y–Ar′–Y═X–Ar array for **3** is therefore dependent upon its redox state and acts as a "molecular switch".

Introduction

Considerable efforts are currently underway to design new molecules whose structures are drastically sensitive to an external stimulus (electrical current, light, etc.) and which could be used as switches in molecular electronics.[1] One strategy for fabricating components for such devices is to support two redox-active species via bridging groups that allow electronic communication between the two redox centers. The various redox states of the system can then lead to different switching states (geometrical changes). Many such potential systems have been constructed, especially those having organometallic and coordination complexes as redox-active partners. For example, a novel diruthenium complex (eq 1) shuttles the geometry of the bridging biphenylene unit by a two-electron redox reaction.[2]

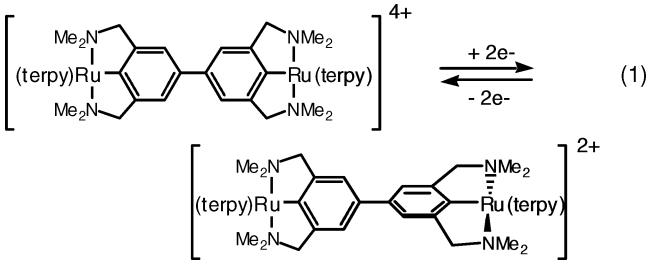

(1)

More recently, systems linking redox-active metal−metal multiply bonded complexes have appeared.[3] These systems thus have access not only to the electrons within the d orbitals

* Authors to whom correspondence should be addressed. E-mail: michel.geoffroy@chiphy.unige.ch (M.G.); jdp5@po.cwru.edu (J.D.P.).
[†] University of Geneva.
[‡] Case Western Reserve University.

(1) (a) Liu, J.; Gomez-Kaifer, M.; Kaifer, A. G. In *Molecular Machines and Motors*; Structure and Bonding; Sauvage, J.-P., Ed.; Springer: Berlin, 2001; pp 142−161. (b) Astruc D. *Electron Transfer and Radical Processes in Transition-Metal Chemistry*; Wiley: New York, 1995. (c) Todres, Z. V. *Organic Ion Radicals, Chemistry and Applications*; Marcel Dekker: New York, 2003.

(2) Steenwinkel, P.; Grove, D. M.; Veldman, N.; Spek, A. L.; Van Koten, G. *Organometallics* **1998**, *17*, 5647.

(3) Fabbrizzi, L.; Licchelli, M.; Pallavicini, P. *Acc. Chem. Res.* **1999**, *32*, 846.

10.1021/ic030079j CCC: $25.00
Published on Web 09/05/2003

of the respective metal centers (type **A**, below) but also to those composing the multiple bonds (π and δ).[4]

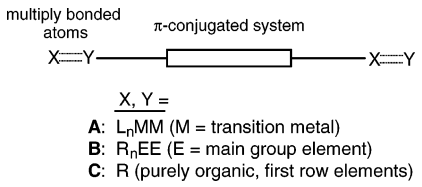

Purely organic systems (type **C**), and their extended oligomeric and polymeric forms, have drawn a lot of attention since their discovery as components of light-emitting diodes and devices.[5] Between these two limits are systems that incorporate multiply bonded main group elements (type **B**); by comparison to **A** or **C**, little work has appeared toward linking multiply bonded main group elements. This fact is odd, as results have shown that molecules containing low-coordinated trivalent phosphorus atoms are easily reduced[6] and could present interesting properties in this context. For example, phosphaalkenes ($RP{=}CR_2$) and diphosphenes (RP═PR), the phosphorus analogues of olefins, are much more easily reduced than olefins owing to the weaker π bonds and the corresponding low lying π^* orbitals in these molecules.[7] In addition, the derived radical anions show significant stability and can be subjected to EPR analyses.

Studies of such systems with extended conjugation pathways have been hampered due to a lack of appropriate synthetic precursors required for their initial construction. Diphosphenes and phosphaalkenes, like many other low-coordinate phosphorus-containing compounds, require stabilizing bulky protective groups. Utilization of the sterically demanding aryl group 2,4,6-tri-*tert*-butylbenzene, Mes*, led to the first successful isolation of a stable diphosphene Mes*P═PMes* in 1981.[8] Since then many sterically encumbered groups have been used to isolate low coordinate main group elements.[9] Most of these systems, including the popular Mes* ligand, place limits on the types of possible multiredox-active systems or extended systems that one can design using such sterically demanding groups. Phosphaalkenes ($RP{=}CR_2$), mixed hybrids of diphosphenes and olefins, have less stringent steric demands for the P═C functional group compared to P═P groups and have provided more opportunities for examining the effect of incorporating multiple numbers of such units in molecules where there can be means for electronic communication between the redox centers.[10] For example, early work showed that diphosphaalkenes having a bridging phenylene (**I**) could be prepared[10f] and their radical anions were studied by EPR.[10h]

Later, Yoshifuji and co-workers successfully prepared a

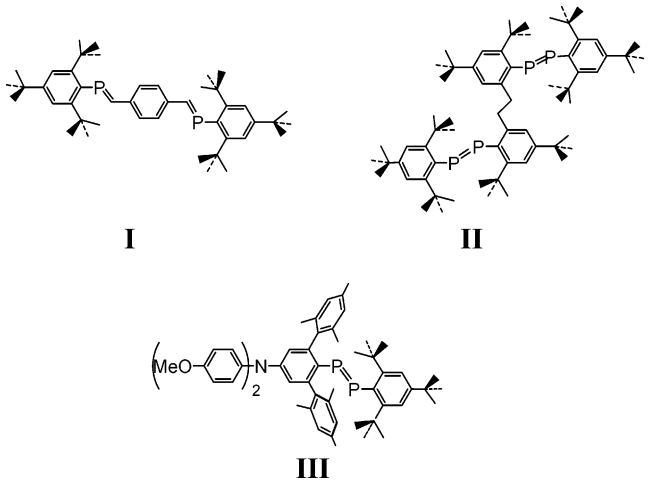

compound having two diphosphene units (**II**).[11] It might be expected that such a molecule having saturated carbon bridges between the redox centers would not allow facile electronic communication between the diphosphenes. More recently molecules have been isolated placing other redox-active groups into possible conjugation with diphosphenes (such as **III**).[12] Such systems are synthetically challenging, and early results show that the impact of the electron-rich diarylamine group upon the electrochemistry of the diphosphene functional unit was minimal.

We have recently prepared new sterically encumbered ligands that provide simultaneous kinetic stability to two low-coordinate phosphorus spanned by a phenylene group.[13] These ligands provide ready access to systems that contain two diphosphene or two phosphaalkene units and have the potential for constructing even larger conjugated systems. In this study, we report EPR data for the reduced forms of the diphosphaalkenes **1** and **2** and of the bis(diphosphene) **3**. To facilitate the interpretation of these spectra, the reduced

(4) Cotton, F. A.; Lin, C.; Murillo, A. *Acc. Chem. Res.* **2001**, *34*, 759.
(5) (a) Wohlgennant, M.; Jiang, X. M.; Vardeny, Z. V.; Janssen, R. A. J. *Phys. Rev. Lett.* **2002**, *88*, 197401. (b) Wohlgennant, M.; Kunj, T.; Mazumdar, S.; Ramasesha, S.; Vardeny, Z. V. *Nature* **2001**, *409*, 494. (c) Segura, J. L.; Martin, N. *J. Mater. Chem.* **2000**, *10*, 2403.
(6) (a) Choua S.; Sidorenkova, H.; Berclaz, T.; Geoffroy, M.; Rosa, P.; Mezailles, N.; Ricard, L.; Mathey, F.; Le Floch, P. *J. Am. Chem. Soc.* **2000**, *122*, 12227. (b) Cataldo, L.; Choua, S.; Berclaz, T.; Geoffroy, M.; Mézailles, N.; Ricard, L.; Mathey, F.; Le Floch, P. *J. Am. Chem. Soc.* **2001**, *123*, 6654. (c) Canac, Y.; Baceiredo, A.; Schoeller, W. W.; Gigmes, D.; Bertrand G. *J. Am. Chem. Soc.* **1997**, *119*, 7579. (d) Loss, S.; Magistrato, A.; Cataldo, L.; Hoffmann, S.; Geoffroy, M.; Röthlisberger, U.; Grützmacher, H. *Angew. Chem., Int. Ed.* **2001**, *40*, 723.
(7) Dillon, K. B.; Mathey, F.; Nixon, J. F. *Phosphorus: The Carbon Copy*; John Wiley and Sons: New York, 1998.
(8) Yoshifuji, M.; Shima, I.; Inamoto, N.; Hirotsu, K.; Higuchi, T. *J. Am. Chem. Soc.* **1981**, *103*, 4587.
(9) (a) Clyburne, J. A. C.; McMullen, N. *Coord. Chem. Rev.* **2000**, *210*, 73. (b) Brothers, P. J.; Power, P. P. In *Multiple Bonded Main Group Metals and Metalloids*; West, R., Stone, F. G., Eds.; Academic Press: San Diego, CA, 1996; pp 1−63. (c) Power, P. P. *J. Chem. Soc., Dalton. Trans.* **1998**, 2939. (d) Twamley, B.; Haubrich, S. T.; Power, P. *Adv. Organomet. Chem.* **1999**, 1. (e) Yoshifuji, M. *J. Chem. Soc., Dalton Trans.* **1998**, 3343. (f) Cowley, A. H.; Norman, N. C. *Prog. Inorg. Chem.* **1986**, *34*, 1. (g) Cowley, A. H. *J. Organomet. Chem.* **1990**, *400*, 71.
(10) (a) Jouaiti, A.; Geoffroy, M.; Terron, G.; Bernardinelli, G. *J. Chem. Soc., Chem. Commun.* **1992**, 155. (b) Jouaiti, A.; Geoffroy, M.; Bernardinelli, G. *Tetrahedron Lett.* **1993**, *34*, 3413. (c) Jouaiti, A.; Geoffroy, M.; Terron, G.; Bernardinelli, G. *J. Am. Chem. Soc.* **1995**, *117*, 2251. (d) Knoch, F.; Appel, R.; Wenzel, H. *Z. Kristallogr.* **1995**, *210*, 450. (e) Jouaiti, A.; Geoffroy, M.; Bernardinelli, G. *J. Chem. Soc., Chem. Commun.* **1996**, 437. (f) Kawanami, H.; Toyota, K.; Yoshifuji, M. *Chem. Lett.* **1996**, 533. (g) Kawanami, H.; Toyota, K.; Yoshifuji, M. *J. Organomet. Chem.* **1997**, *535*, 1. (h) Al Badri, A.; Jouaiti, A.; Geoffroy, M. *Magn. Reson. Chem.* **1999**, *37*, 735.
(11) Yoshifuji, M.; Shinohara, N.; Toyota, K. *Tetrahedron Lett.* **1996**, *37*, 7815.
(12) Tsuji, K.; Sasaki, S.; Yoshifuji, M. *Tetrahedron Lett.* **1999**, *40*, 3203.
(13) Shah, S.; Concolino, T.; Rheingold, A. L.; Protasiewicz, J. D. *Inorg. Chem.* **2000**, *39*, 3860.

form of the asymmetric diphosphene DmpP═PMes* (**4**)[14] has also been investigated by EPR. Comparison to previous results obtained for the reduction of the related diphosphene **5** are also presented.

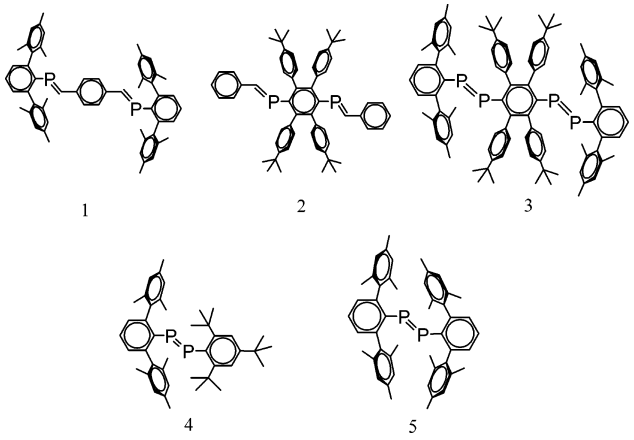

These data, in conjunction with DFT calculations, show how a subtle interplay between steric and electronic preferences can induce geometrical changes depending on the overall redox state of a material. The present work shows that the relative importance of these two opposing forces can interchange upon successive reductions and thus give rise to properties akin to a "molecular switch".

Experimental Section

Compounds **2**−**5** were prepared as previously described.[13,14]

Synthesis of DmpP═C(H)C$_6$H$_4$C(H) ═PDmp (1). To 0.200 g (0.476 mmol) of DmpP═PMe$_3$ in 20 mL of THF was added 1.00 equiv (32.0 mg, 0.238 mmol) of 1,4-terephthaldehyde. The reaction mixture was allowed to stir for 5 h during the course of which increasing amounts of yellow precipitate is formed. Upon removal of THF under vacuum, the crude reaction mixture was dissolved in about 50 mL of hot toluene and recrystallized at −35 °C to afford diphosphaalkene **1** as light-yellow flakes (0.135 g, 40.0% yield). Mp: 241−243 °C. ^{31}P{^{1}H} NMR (C$_6$D$_6$): δ 243.5. ^{1}H NMR (C$_6$D$_6$): δ 8.71 (d, $^2J_{HP}$ = 23.7 Hz, 2H), 7.18 (t, J_{HH} = 7.5 Hz, 2H), 6.96 (d, J_{HH} = 7.5 Hz, 4H), 6.78 (s, 8H), 6.65 (s, 4H), 2.15 (s, 24H), 2.07 (s, 12H). HRMS (EI) (*m*/z): calcd for $C_{56}H_{56}P_2$, 790.3811; found, 790.3899.

EPR. The spectra were recorded on Bruker 200D-SRC and Bruker ESP-300 spectrometers (X-band, 100 kHz field modulation) equipped with a variable-temperature attachment. Freshly distilled solvents were used for the preparation of all samples, and solutions were carefully degassed. The electrochemical generation of the radical anions was performed by in situ electrolysis in the EPR cavity using platinum electrodes and tetrabutylammonium hexafluorophosphate (0.1M) as an electrolyte together with a Princeton Applied Research potentiostat. Chemical reductions with sodium (or potassium) were performed under high vacuum (10^{-5} Torr) by reacting a solution of the organophosphorus compound in THF on a sodium (or potassium) mirror. Chemical reductions with sodium naphthalenide were carried out in a glovebox; after reaction the solutions (10^{-2} M in THF) were kept under nitrogen atmosphere and rapidly studied by EPR.

DFT Calculations. Quantum calculations were carried out on a Silicon Graphics workstation with the Gaussian 98 package[15] using B3LYP functional[16] together with the 6-31G* basis set for the neutral systems and the 6-31+G* basis set for the anionic ones. Some additional calculations were also performed by using the TZVP[17] and the IGLO-III[18] basis sets; the corresponding results are given as Supporting Information. The optimized geometries were characterized by harmonic frequency analysis as minima (all frequencies real). The molecular orbitals were represented with the Molekel program[19] by carrying out a single-point restricted-DFT calculation at the optimized geometry.

Electrochemistry. Tetrabutylammonium tetrafluoroborate was recrystallized twice from hot ethyl acetate and dried under vacuum at 130−140 °C for 2−3 h. The experiments were performed inside a nitrogen-filled Vacuum Atmospheres drybox using a conventional three-electrode cell, a model RDE 3 Pine Instruments potentiostat, and a Houston Instruments X−Y recorder. A glassy carbon working electrode (approximate area, 0.070 cm^2, BAS) was used for the cyclic voltammetry experiments whereas a platinum gauze electrode (area, 10 cm^2) was used for the bulk electrolysis. Silver wire was used as a quasi-reference electrode, and a platinum wire was the counter electrode. The purity of the solutions was verified by running background voltammograms. Samples studied by cyclic voltammetry were prepared using 10 mL of THF, 0.1 M in the supporting electrolyte (tetrabutylammonium tetrafluoroborate) and 0.001 M in the bis(diphosphene). All potentials were corrected to SCE using the Fc$^+$/Fc couple.

Results

Formation and EPR Spectra of Radical Anions. The ease of reduction of phosphaalkenes[10a,c,h,20] and diphosphenes[21] to stable anions relative to their all-carbon counterparts (olefins) is well established. Owing to the relatively low-lying π* LUMOs in these materials, addition of an electron to the π* orbital is not very difficult. Additionally, as many of these materials bear sterically demanding groups, the resulting radical anions are often persistent at ambient conditions in the absence of air or water. In general, diphosphenes are more readily reduced than analogous

(14) Smith, R. C.; Urnezius, E.; Lam, K.-C.; Rheingold, A. L.; Protasiewicz, J. D. *Inorg. Chem.* **2002**, *41*, 5296.

(15) Frisch, M. J.; Trucks, G. W.; Schlegel, H. B.; Scuseria, G. E.; Robb, M. A.; Cheeseman, J. R.; Zakrzewski, V. G.; Montgomery, J. A.; Stratmann, R. E.; Burant, J. C.; Dapprich, S.; Millam, J. M.; Daniels, A. D.; Kudin, K. N.; Strain, M. C.; Farkas, O.; Tomasi, J.; Barone, V.; Cossi, M.; Cammi, R.; Mennucci, B.; Pomelli, C.; Adamo, C.; Clifford, S.; Ochterski, J.; Petersson, G. A.; Ayala, P. Y.; Cui, Q.; Morokuma, K.; Malick, D. K.; Rabuck, A. D.; Raghavachari, K.; Foresman, J. B.; Cioslowski, J.; Ortiz, J. V.; Stefanov, B. B.; Liu, G.; Liashenko, A.; Piskorz, P.; Komaromi, I.; Gomperts, R.; Martin, R. L.; Fox, D. J.; Keith, T.; Al-Laham, M. A.; Peng, C. Y.; Nanayakkara, A.; Gonzalez, C.; Challacombe, M.; Gill, P. M. W.; Johnson, B. G.; Chen, W.; Wong, M. W.; Andres, J. L.; Head-Gordon, M.; Replogle, E. S.; Pople, J. A. *Gaussian 98 (Revision A.7)*; Gaussian, Inc.: Pittsburgh, PA, 1998.

(16) Becke, A. D. *J. Chem. Phys.* **1993**, *98*, 5648.

(17) Godbout, N.; Salahub, D. R.; Andzelm, J.; Wimmer, E. *Can. J. Chem.* **1992**, *70*, 560.

(18) Kutzelnigg, W.; Fleischer, U.; Schindler, M. In *NMR: Basic Principles and Progress*; Springer-Verlag: Berlin, 1990; Vol. 23, p 165.

(19) Flukiger, P. Development of Molecular Graphics Package MOLEKEL. Ph.D. Thesis, University of Geneva, Geneva, Swizerland, 1992.

(20) Geoffroy, M.; Jouaiti, A.; Terron, G.; Cattani-Lorente, M.; Ellinger, Y. *J. Phys. Chem.* **1992**, *96*, 8241.

(21) (a) Cetinkaya, B.; Hudson, A.; Lappert, M. F.; Goldwhite, H. *J. Chem. Soc., Chem. Commun.* **1982**, 609. (b) Bard, A. J.; Cowley, A. H.; Kilduff, J. E.; Leland, J. K.; Norman, N. C.; Palkuvski, M. *J. Chem. Soc., Dalton Trans.* **1987**, 249. (c) Culcasi, M.; Grouchi, G.; Escudié, J.; Couret, C.; Pujol, L.; Tordo, P. *J. Am. Chem. Soc.* **1986**, *108*, 3130.

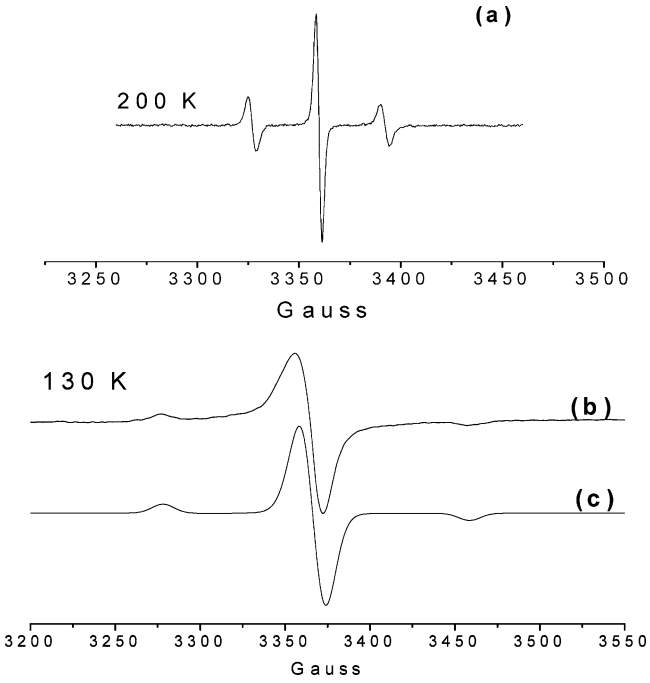

Figure 1. EPR spectra of $\mathbf{1}^{\bullet-}$ (a) at 200 K and (b) at 130 K and (c) simulation of the frozen solution spectrum.

Table 1. Experimental EPR Tensors[a] and Phosphorus Spin Densities for $\mathbf{1}^{\bullet-}$

g tensor	^{31}P coupling tensors (MHz)	^{31}P anisotropic and isotropic coupling (MHz)	phosporus atomic spin densities
$g_x = 2.0045$	$T_\perp = 20$	$\tau_\perp = -77$	$\rho_p = 0.21$
$g_y = 2.0048$	$T_z = 252$	$\tau_\parallel = 155$	$\rho_s = 0.007$
$g_z = 2.0025$		$A_{iso} = 97$	

[a] From frozen solution spectra.

phosphaalkenes. Furthermore, the radical anions derived from reduction of diphosphenes tend to show more stability than the radical anions derived from reduction of phosphaalkenes. These generalizations were also found to be true for bis(diphosphene) **3** compared to **1** and **2**. Reductions of **1**−**3** were thus undertaken to assess the degree of delocalization of the unpaired spin over the two possible electron acceptor sites.

EPR Spectra of $\mathbf{1}^{\bullet-}$. Electrochemical reduction (room temperature) or chemical reduction (200 K) by Na naphthalenide or K mirror of THF solutions of **1** produce solutions of radical anion $\mathbf{1}^{\bullet-}$ that are EPR active. The spectra recorded at 200 K (Figure 1a) exhibit hyperfine coupling with two equivalent ^{31}P nuclei (92 MHz). Decreasing temperature causes a drastic broadening of the lines. The hyperfine structure observed at 130 K on the frozen solution spectrum (Figure 1b) is characteristic of two aligned axial ^{31}P tensors.

This spectrum has been simulated (Figure 1c) by adjusting the dipolar couplings and by assuming that the isotropic coupling remains almost invariant ($A_{iso}(^{31}P) = 97$ MHz in the solid state). The resulting principal values and their decomposition into isotropic and anisotropic coupling constants are given in Table 1, together with the spin densities deduced from a comparison with atomic coupling constants.[22]

(22) Morton, J. R.; Preston, K. F. *J. Magn. Reson.* **1978**, *30*, 577.

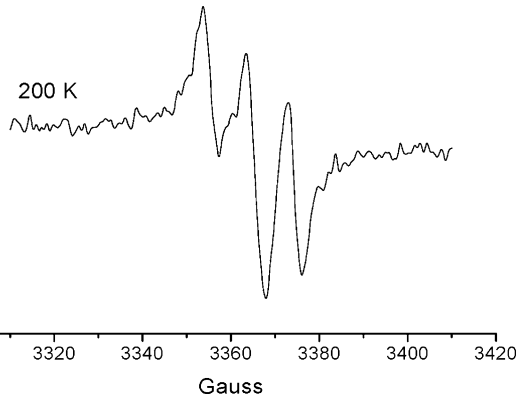

Figure 2. EPR spectrum of $\mathbf{2}^{\bullet-}$ at 200 K.

Similar spectra are also observed by reduction of **1** on a sodium mirror in the presence of a crown ether (18-crown-6). Analysis of these spectra are complicated by the presence of an additional signal in the central part of the spectrum, which may be due to a degradation compound.

EPR Spectra of $\mathbf{2}^{\bullet-}$. The EPR spectrum obtained after electrochemical reduction of a solution of **2** in THF (8×10^{-3} M) at 200 K is shown in Figure 2. It is characterized by a hyperfine coupling of 28 MHz with two equivalent spin-1/2 nuclei. Above 230 K the intensity decreases. The spectrum obtained after freezing of the solution broadens (peak to peak width $\cong$ 20 G) but is composed of a single band. The slightly orange solution obtained after reaction at 200 K of a solution of **2** in THF on a potassium mirror leads also to three peaks separated by 28 MHz. Similar results were obtained by reaction on a Na mirror in the presence of crown ether.

EPR Spectra of $\mathbf{3}^{\bullet-}$ and $\mathbf{3}^{2-}$. Reduction of THF solutions of **3** to $\mathbf{3}^{\bullet-}$ was readily achieved by a variety of means that include electrochemical reduction, chemical reduction at 200 K on a Na mirror in the presence of crown ether, or reduction with Na naphthalenide in the presence of crown ether. Regardless of the method used, at room temperature, the resulting EPR spectra (Figure 3a) are similar and are composed of a triplet ($A_{iso} = 98$ MHz) of triplets ($A_{iso} = 25$ MHz). The spectrum obtained by using Na naphthalenide as a reductant is particularly intense, and at 130 K it yields the frozen solution spectrum shown in Figure 3b. This spectrum is rather complex and has been analyzed by assuming that the isotropic coupling constants were only slightly sensitive to temperature. The resulting EPR tensors, given in Table 2, lead to a simulated spectrum which is quite similar to the experimental one (Figure 3c). The tensors exhibit axial symmetry, and their "parallel" components are aligned in a common direction. Their decomposition in isotropic and anisotropic coupling constants is given in Table 2 together with the corresponding spin densities.

Reduction of **3** with 2 equiv of Na{18-C-6} naphthalenide led to a paramagnetic species whose EPR spectrum is shown in Figure 4a. This spectrum exhibits isotropic coupling constants with two inequivalent ^{31}P nuclei, $A_1 = 173$ MHz and $A_2 = 78$ MHz; probably due to molecular motion the four line widths are not equal. The corresponding frozen

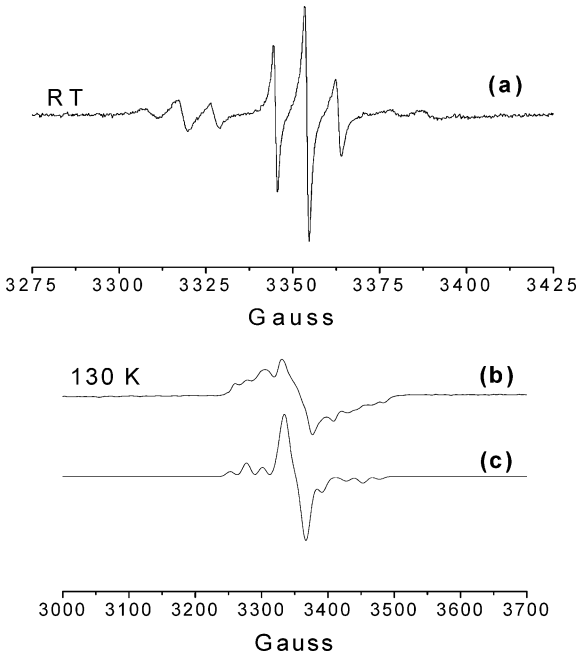

Figure 3. EPR spectra of $\mathbf{3}^{\bullet-}$ (a) at RT (room temperature) and (b) at 130 K and (c) simulation of the frozen solution spectrum.

Table 2. Experimental EPR Tensors[a] and Phosphorus Spin Densities for $\mathbf{3}^{\bullet-}$

	^{31}P coupling tensors (MHz)		^{31}P anisotropic and isotropic coupling (MHz)		phosphorus spin densities	
g tensor	P1 (2×)	P2 (2×)	P1 (2×)	P2 (2×)	P1 (2×)	P2 (2×)
$g_\perp = 2.014$	$T_\perp = 22$	$T_\perp = 11$	$\tau_\perp = -74$	$\tau_\perp = 20$	$\rho_p = 0.195$	$\rho_p = 0.053$
$g_\parallel = 2.0032$	$T_\parallel = 243$	$T_\parallel = 70$	$\tau_\parallel = 147$	$\tau_\parallel = 39$	$\rho_s = 0.007$	$\rho_s = 0.002$
			$A_{iso} = 96$	$A_{iso} = 31$		

[a] From frozen solution spectra.

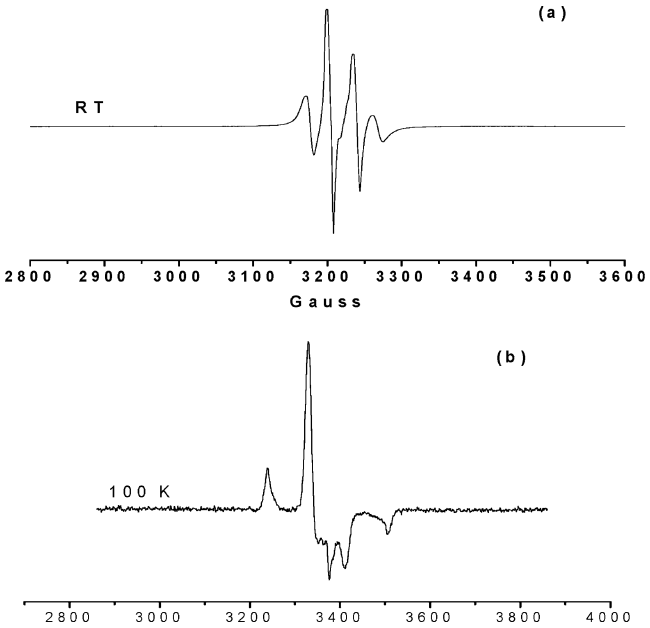

Figure 4. EPR spectra of $\mathbf{3}^{2-}$ (a) at RT and (b) at 100 K.

solution spectrum, obtained at 100 K, is shown in Figure 4b; it does not exhibit a forbidden transition ($\Delta M_s = 2$) at half-field which is a typical feature for most triplet diradicals.

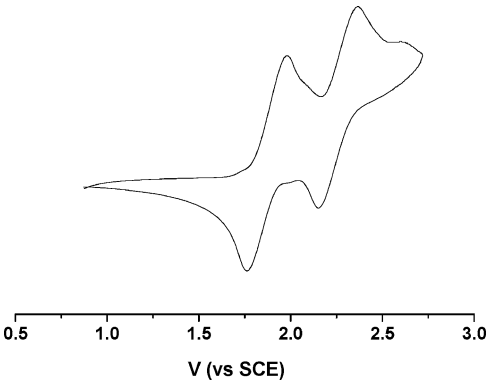

Figure 5. Cyclic voltammetry of a solution of **3**.

Additional information about the doubly reduced product is yielded by cyclic voltammetry. The voltammogram of THF solutions of **3** is shown in Figure 5 and is compared to the CV of the related monofunctional diphosphene analogue **5** (DmpP═PDmp, Dmp = 2,6-$Mes_2C_6H_3$).[23]

Several points are noteworthy. First, there are indeed two reversible one electron redox processes for **3**. The potentials for these two processes bracket the potential observed for **5**. The fact that two such waves are observed indicate substantial electronic coupling of the two redox centers in **3**. The extent of conjugation, or the electronic delocalization, between the two equivalent P═P units in **3** can be gauged by the comproportionation constant K_{com} [1b,24] for the following equilibrium: This value can be computed from the

$$[\mathbf{3}]^{2-} + 3 \underset{}{\overset{K_{com}}{\rightleftharpoons}} 2\,[\mathbf{3}]^{\bullet-}$$

difference in potentials $E_{1/2}(0/1-)$ and $E_{1/2}(1-/2-)$ by the expression $K_{com} = \exp\{F[E_{1/2}(0/1-) - E_{1/2}(1-/2-)]/RT\}$. The difference in potential of 340 mV leads to a value of K_{com} of 5.6×10^5. Such interpretations, however, have been recently shown to be susceptible to complicating medium effects.[25] Regardless, the fact that we can independently generate and characterize each reduction product by EPR spectroscopy minimally indicates a large and significant value for K_{com}.

In addition, the CV data suggest that **3** is more readily reduced than DmpP═PDmp (**5**) and that **3** should be chemically reduced by the anion $\mathbf{5}^{\bullet-}$. Indeed, $\mathbf{3}^{\bullet-}$ is cleanly produced by the action of $\mathbf{5}^{\bullet-}$ on **3**. Furthermore, addition of excess $\mathbf{5}^{\bullet-}$ to **3** does not form $[\mathbf{3}]^{2-}$. Finally, careful analysis of the CV data shows the presence of a small amount of a second redox-active species, as discerned by small shoulders or irregularities riding on the waves. While ^{31}P NMR studies of **3** do not show evidence for anything but a bis-*E*-configured bis(diphosphene) having P═P units located above and below the central benzene ring (as also observed for the X-ray structure of **3**), calculations on the model bis(diphosphene) PhP═PC_6H_4P═PPh (**3′**) show that two con-

(23) Shah, S.; Burdette, S. C.; Swavey, S.; Urbach, F. L.; Protasiewicz, J. D. *Organometallics* **1997**, *16*, 3395.
(24) (a) Creutz, C. *Prog. Inorg. Chem.* **1983**, *30*, 1. (b) Nelsen, S. F. *Chem. Eur. J.* **2000**, *6*, 581.
(25) Barriere, F.; Camire, N.; Geiger, W. E.; Mueller-Westerhoff, U. T.; Sanders, R. *J. Am. Chem. Soc.* **2002**, *124*, 7262.

Table 3. Experimental EPR Tensors[a] and Phosphorus Spin Densities for $4^{\bullet-}$

g tensor	^{1}H coupling (MHz)	^{31}P coupling tensors (MHz)		^{31}P anisotropic and isotropic coupling (MHz)		phosphorus spin densities	
		P1	P2	P1	P2	P1	P2
$g_{\perp 1} = 2.0036$	$T_\perp = -25$	$T_\perp = 74$	$T_\perp = -2.4$	$\tau_\perp = -122.5$	$\tau_\perp = -126$	$\rho_p = 0.43$	$\rho_p = 0.315$
$g_{\perp 2} = 2.0015$	$T_{\|\|} = 52$	$T_\perp = -0.4$	$T_\perp = 19$	$\tau_\perp = -196.9$	$\tau_\perp = -104.5$	$\rho_s = 0.01$	$\rho_s = 0.009$
$g_{\|\|} = 2.023$		$T_{\|\|} = 516$	$T_{\|\|} = 354$	$\tau_{\|\|} = 319.5$	$\tau_{\|\|} = 230.5$		
	$A_{iso} = 0$			$A_{iso} = 196.5$	$A_{iso} = 123.5$		

[a] From frozen solution spectra.

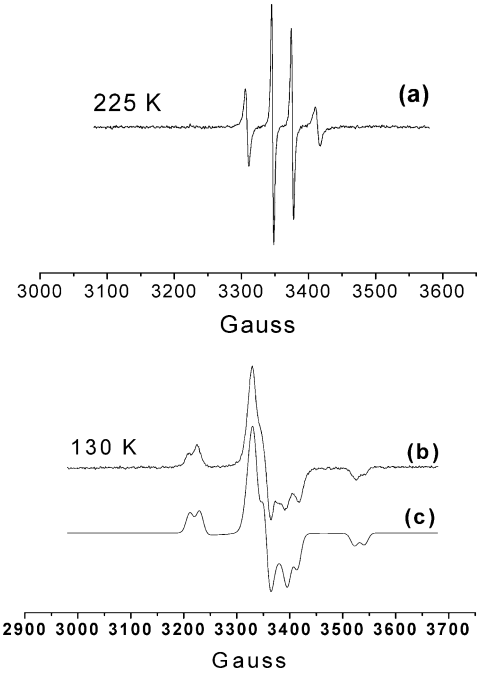

Figure 6. EPR spectra of $4^{\bullet-}$ (a) at 225 K and (b) at 130 K and (c) simulation of the frozen solution spectrum of $4^{\bullet-}$.

formers ($\mathbf{3'_a}$ and $\mathbf{3'_b}$; vide infra) have similar energies. A second conformer might give rise to the additional complexity of the CV data, but since it is present in very low concentration and is not detected by other experiments, this explanation is tentative at this time.

EPR Spectra of $4^{\bullet-}$. In the presence of Na and 18-crown-6, a solution of **4** in THF leads, at 225 K, to the EPR spectrum shown in Figure 6a. This spectrum is characterized by two different isotropic coupling constants: $A_1(^{31}P) = 204$ MHz; $A_2(^{31}P) = 95$ MHz. The intensity distribution is affected by the reorientation of the radical anion. The frozen solution spectrum obtained at 130 K is shown in Figure 6b; it can be simulated (Figure 6c) by using the tensors shown in Table 3. The ^{31}P anisotropic coupling constants correspond to two appreciably different phosphorus spin densities (ρ(P1) = 0.4, ρ(P2) = 0.32). The proton hyperfine coupling detected, on the frozen solution spectrum, by the splitting of the external lines is essentially dipolar. It indicates that a hydrogen atom of a protective group (most likely from Mes* group) is probably located close to the magnetic orbital of one of the two phosphorus atoms and confirms the steric constraints or pressures present in the radical anion.[26]

DFT Calculations. The size of molecules mentioned above is far too large to expect quantitative results from the available nonempirical methods. DFT calculations were performed on model systems, to characterize the molecular structures and electronic properties in absence of steric constraints imposed by large substituents.

Table 4. Optimized Geometries (Å, deg) for the Two Conformers of **1′** and Their Radical Anions

params	$\mathbf{1'_a}$	$\mathbf{1'_b}$	$\mathbf{1'_a}^{\bullet-}$	$\mathbf{1'_b}^{\bullet-}$
P_a-C_a	1.699	1.698	1.742	1.743
C_a-C_1	1.453	1.453	1.420	1.421
$C_{1a}-P_a$	1.837	1.838	1.838	1.838
$C_{2a}-C_{3a}$	1.394	1.395	1.397	1.397
C_1-C_2	1.413	1.410	1.433	1.431
C_2-C_3	1.384	1.388	1.378	1.376
$C_a-P_a-C_{1a} = \theta_2$	102.95	102.95	103.03	102.75
$P_a-C_a-C_1 = \theta_1$	126.56	126.59	127.35	127.27
$C_a-P_a-C_{1a}-C_{2a} = \xi_2$	−34.3	−4.2	−24.5	−26.8
$C_1-C_a-P_a-C_{1a}$	−178.1	-178.2	175.9	174.9
$C_6-C_1-C_a-P_a = \xi_1$	−5.2	−4.3	−4.0	−5.3
$n(C_2C_1C_6),n(C_{2a}C_{1a}C_{6a})$	37.6	38.25	28.71	32.18

Diphosphaalkene 1′. The geometries of the model molecules **1′**, as well as those of the corresponding radical monoanions, were optimized by DFT. The geometries for the two conformers $\mathbf{1'_a}$ and $\mathbf{1'_b}$ are shown in Table 4, while the hyperfine couplings of the monoanions are shown in Table 5. The two conformers have practically the same energy ($E(\mathbf{1'_b}) - E(\mathbf{1'_a}) = 0.06$ kcal, $E([\mathbf{1'_a}]^{\bullet-}) - E([\mathbf{1'_b}]^{\bullet-}) = 0.21$ kcal), and their coupling constants are very similar.

Diphosphaalkene 2′. Optimization of the model molecules

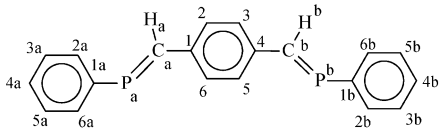

$\mathbf{1'_a}$

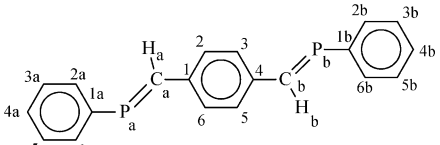

$\mathbf{1'_b}$

2′ led to the two conformers $\mathbf{2'_a}$ and $\mathbf{2'_b}$ whose geometric parameters are given in Table 6 together with those obtained from the crystal structure of **2** and those calculated for the monoanions. For both the neutral and the anionic species the energy difference between the two isomers is again less than 1 kcal mol^{-1}.

The hyperfine couplings predicted by DFT for $\mathbf{2'_a}^{\bullet-}$ and $\mathbf{2'_b}^{\bullet-}$ are given in Table 7; they are practically the same for

(26) Smith, R. C.; Shah, S.; Urnezius, E.; Protasiewicz, J. D. *J. Am. Chem. Soc.* **2003**, *125*, 40.

Table 5. Hyperfine Couplings for $\mathbf{1'_a}^{\bullet-}$ and $\mathbf{1'_b}^{\bullet-}$

	isotropic couplings (MHz)		anisotropic couplings (MHz)	
$\mathbf{1'_a}^{\bullet-}$	$P_a = P_b = 50.12$	$H_a = H_b = -3.59$	$\tau_\perp(P_a) = \tau_\perp(P_b) = -89.04$ $\tau_\perp(P_a) = \tau_\perp(P_b) = -82.40$ $\tau_{||}(P_a) = \tau_{||}(P_b1) = 171.44$	$\tau_i(H_a) = \tau_i(H_b) = -1.68$ $\tau_j(H_a) = \tau_j(H_b) = -1.81$ $\tau_k(H_a) = \tau_k(H_b) = 3.49$
$\mathbf{1'_b}^{\bullet-}$	$P_a = P_b = 54.26$	$H_a = H_b = -4.14$	$\tau_\perp(P_a) = \tau_\perp(P_b) = -88.17$ $\tau_\perp(P_a) = \tau_\perp(P_b) = -81.48$ $\tau_{||}(P_a) = \tau_{||}(P_b) = 169.65$	$\tau_i(H_a) = \tau_i(H_b) = -1.71$ $\tau_j(H_a) = \tau_j(H_b) = -2.25$ $\tau_j(H_a) = \tau_{||}(H_b) = 3.96$

Table 6. Optimized Geometries (Å, deg) for Two Planar Conformations of the Neutral Diphosphaalkene **2′** and of Its Radical Anion $\mathbf{2'}^{\bullet-}$

params	$\mathbf{2'_a}$	$\mathbf{2'_b}$	$\mathbf{2_b}$ (crystal)	$\mathbf{2'_a}^{\bullet-}$	$\mathbf{2'_b}^{\bullet-}$
C_a-P_a	1.696	1.697	1.676	1.726	1.725
P_a-C_1	1.836	1.837	1.848	1.801	1.801
C_a-C_{1a}	1.459	1.459	1.453	1.446	1.445
$C_{1a}-C_{2a}$	1.412	1.412	1.408	1.423	1.423
C_2-C_3	1.392	1.393	1.404	1.385	1.384
C_1-C_2	1.406	1.408	1.407	1.423	1.421
$P_a-C_a-C_{1a} = \theta_2$	126.7	126.67	124.8	125.73	125.81
$C_a-P_a-C_1 = \theta_1$	102.91	102.84	101.43	106.65	106.49
$P_a-C_a-C_{1a}-C_{2a} = \xi_2$	−5.7	−5.6	−22.5	0.0	0.0
$C_1-P_a-C_a-C_{1a}$	178.0	178.2	172.1	−179.4	180.0
$C_6-C_1-P_a-C_a = \xi_1$	−34.4	−34.2	68.9	1.6	0.0
$n(C_2C_1C_6)$,$n(C_{2a}C_{1a}C_{6a})$	48.87	38.40	68.0	3.88	179.98

the two conformers.

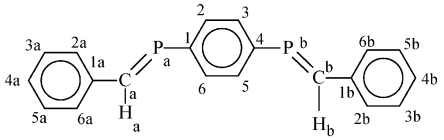

$\mathbf{2'_a}$

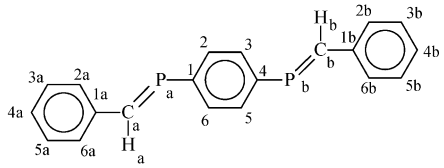

$\mathbf{2'_b}$

Bis(diphosphene) 3′. Calculations were carried out on the two isomers $\mathbf{3'_a}$ and $\mathbf{3'_b}$, as well as on the two corresponding isomers of $HP{=}PC_6H_4P{=}PH$ ($\mathbf{3''_a}$ and $\mathbf{3''_b}$).

The optimized geometries are reported in Table 8 together with those calculated for the corresponding radical anions. The two neutral conformers have similar energies ($E(\mathbf{3'_b}) - E(\mathbf{3'_a}) = -0.41$ kcal), as well as the two radical conformers ($\Delta E = -0.38$ kcal). The calculated hyperfine couplings are reported in Table 9; they are practically the same for the two conformers.

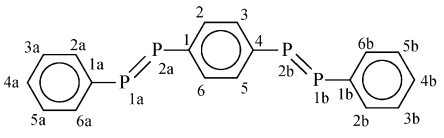

$\mathbf{3'_a}$

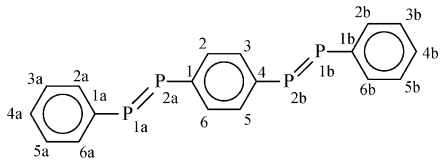

$\mathbf{3'_b}$

The geometries of the dianion $[\mathbf{3_b'}]^{2-}$ have been optimized for the singlet and triplet state; the corresponding parameters are reported in Table 10. The most stable structure is found for the singlet state in its planar conformation. The lowest triplet state corresponds to a nonplanar conformation ($\xi_1 = 21.7°$) of the dianion. It lies 2.3 kcal mol^{-1} above the singlet ground state, and its energy is very slightly smaller than that of the triplet state in a planar conformation ($E_{T,p} - E_{T,np} = 0.1$ kcal mol^{-1}); the energy of the nonplanar singlet is 18.9 kcal mol^{-1} higher than that of the planar triplet. This relative position of the singlet ground state (planar structure) and of the triplet state (twisted structure) is reminiscent of that found for bis(verdazyl) diradicals [27] ($E_{T,np} - E_{S,p} = 2.2$ kcal mol^{-1} (760 cm^{-1})).

Discussion

Singly Reduced Difunctional Materials. In the absence of any protective group, the main structural features on the system $[Ph-X{=}Y-C_6H_4-Y{=}X-Ph]^{\bullet-}$, where Y or X represents P or CH, can be obtained from the DFT results reported in Tables 4, 6, and 8. For the three model compounds, **1′**, **2′**, and **3′**, the C1a,X,Y,C1 (or C1b,X,Y,C4) atoms are almost coplanar. The general geometry of the molecule can be characterized by the dihedral angle ξ_1 between this C1a,X,Y,C1 (or C1b,X,Y,C4) plane and the central benzene ring and by the dihedral angle ξ_2 between the C1a,X,Y,C1 (or C1b,X,Y,C4) plane and the external aromatic ring (Chart 1).

For the three model compounds (**1′**−**3′**), the θ_1 and θ_2 bond angles are close to 103° for CPY and XPC, whereas they are close to 125° for CCY or XCC. Moreover, whereas the dihedral angle ξ_1 is close to 0° or 180° for **1′** (where Y represents the CH group), this dihedral angle opens to 32° for **2′** and **3′** (when Y represents P). Similarly, the ξ_2 dihedral angle is close to 0° for **2′** (where X represents the CH group) and close to 33° for **1′** and **3′** (where X is a phosphorus atom). The out-of-plane movement by ∼32° probably reveals an interaction between the phosphorus lone pair and the C−H bond of the neighboring phenyl ring. Moreover, the bond angles at the phosphorus atom being more acute (ca. 103° versus 120° for CH group), the interaction of the X=Y unit with ortho hydrogens is stronger for the benzene ring bound to the phosphorus atom than for the ring bound to the carbon atom; this interaction is minimized when the X=Y bond is not coplanar with benzene ring attached to the phosphorus atom.

(27) Chung, G.; Lee, D. *Chem. Phys. Lett.* **2001**, *350*, 339.

Table 7. Calculated Hyperfine Couplings for $\mathbf{2'_a}^{\bullet-}$ and $\mathbf{2'_b}^{\bullet-}$

	isotropic couplings (MHz)		anisotropic couplings (MHz)	
$\mathbf{2'_a}^{\bullet-}$	$P_a = P_b = 2.14$	$H_a = H_b = -16.33$	$\tau_\perp(P_a) = \tau_\perp(P_b) = -16.43$	$\tau_i(H_a) = \tau_i(H_b) = -1.35$
			$\tau_\perp(P_a) = \tau_\perp(P_b) = -18.50$	$\tau_j(H_a) = \tau_j(H_b) = -8.12$
			$\tau_{\|\|}(P_a) = \tau_{\|\|}(P_b) = 34.94$	$\tau_k(H_a) = \tau_k(H_b) = 9.46$
$\mathbf{2'_b}^{\bullet-}$	$P_a = P_b = 2.07$	$H_a = H_b = -16.22$	$\tau_\perp(P_a) = \tau_\perp(P_b) = -17.18$	$\tau_i(H_a) = \tau_i(H_b) = -1.30$
			$\tau_\perp(P_a) = \tau_\perp(P_b) = -19.23$	$\tau_j(H_a) = \tau_j(H_b) = -7.92$
			$\tau_{\|\|}(P_a) = \tau_{\|\|}(P_b) = 36.41$	$\tau_k(H_a) = \tau_k(H_b) = 9.22$

Table 8. Calculated Geometries (Å, deg) for Neutral and Monoanionic Bis(diphosphenes)

params	$\mathbf{3'_a}$	$\mathbf{3''_a}$	$\mathbf{3'_b}$	$\mathbf{3''_b}$	$\mathbf{3}_b$ (cryst)	$\mathbf{3'_a}^{\bullet-}$	$\mathbf{3''_a}^{\bullet-}$	$\mathbf{3'_b}^{\bullet-}$	$\mathbf{3''_b}^{\bullet-}$
$P_{1a}-P_{2a}$	2.059	2.054	2.060	2.053	2.009	2.108	2.109	2.107	2.108
$P_{2a}-C_1$	1.835	1.837	1.835	1.837	1.854	1.801	1.799	1.802	1.799
$C_{1a}-P_{1a}$	1.835	1.427	1.835	1.427	1.843	1.843	1.433	1.843	1.433
$C_{1a}-C_{2a}$	1.40		1.409		1.400	1.413		1.414	
C_2-C_3	1.390	1.390	1.391	1.392	1.402	1.384	1.384	1.385	1.383
C_1-C_2	1.410	1.412	1.408	1.412	1.407	1.422	1.423	1.420	1.423
$P_{2a}-P_{1a}-C_{1a} = \theta_2$	102.13	91.97	102.27	91.96	106.30	102.73	91.50	102.80	91.63
$P_{1a}-P_{2a}-C_1 = \theta_1$	101.96	109.08	102.03	105.07	97.52	104.95	106.34	104.67	106.02
$C_1-P_{2a}-P_{1a}-C_{1a}$	175.43	−179.9	175.25	179.9	−172.50	180.00	180.00	179.95	179.96
$C_6-C_1-P_{2a}-P_{1a} = \xi_1$	149.78	179.9	150.99	0.00	-84.3 0	0.00	0.00	179.79	0.05
$n(C_2C_1C_6)$,$n(C_{2a},C_{1a},C_{6a})$	115.02		117.50		111.94	179.95		179.71	
$C_{2a}-C_{1a}-P_{1a}-P_{2a} = \xi_2$	32		−32.0		−46.3	0.0		0.1	

Table 9. Calculated ^{31}P Hyperfine Couplings for the Radical Anions $\mathbf{3'}^{\bullet-}$ and $\mathbf{3''}^{\bullet-}$

	^{31}P isotropic couplings (MHz)		^{31}P anisotropic couplings (MHz)	
$\mathbf{3'_a}^{\bullet-}$	$P_{1a} = P_{1b} = 49.47$	$P_{2a} = P_{2b} = 13.35$	$\tau_\perp(P_{1a}) = \tau_\perp(P_{1b}) = -97.5$	$\tau_\perp(P_{2a}) = \tau_\perp(P_{2b}) = -25.71$
			$\tau_\perp(P_{1a}) = \tau_\perp(P_{1b}) = -91.8$	$\tau_\perp(P_{2a}) = \tau_\perp(P_{2b}) = -24.17$
			$\tau_{\|\|}(P_{1a}) = \tau_{\|\|}(P_{1b}) = 189.34$	$\tau_{\|\|}(P_{2a}) = \tau_{\|\|}(P_{2b}) = 49.88$
$\mathbf{3'_b}^{\bullet-}$	$P_{1a} = P_{1b} = 47.37$	$P_{2a} = P_{2b} = 13.66$	$\tau_\perp(P_{1a}) = \tau_\perp(P_{1b}) = -90.18$	$\tau_\perp(P_{2a}) = \tau_\perp(P_{2b}) = -25.27$
			$\tau_\perp(P_{1a}) = \tau_\perp(P_{1b}) = -95.83$	$\tau_\perp(P_{2a}) = \tau_\perp(P_{2b}) = -26.86$
			$\tau_{\|\|}(P_{1a}) = \tau_{\|\|}(P_{1b}) = 186.01$	$\tau_{\|\|}(P_{2a}) = \tau_{\|\|}(P_{2b}) = 52.13$
$\mathbf{3''_a}^{\bullet-}$	$P_{1a} = P_{1b} = 42.9$	$P_{2a} = P_{2b} = 17.12$	$\tau_\perp(P_{1a}) = \tau_\perp(P_{1b}) = -104.2$	$\tau_\perp(P_{2a}) = \tau_\perp(P_{2b}) = -32.42$
			$\tau_\perp(P_{1a}) = \tau_\perp(P_{1b}) = -97.9$	$\tau_\perp(P_{2a}) = \tau_\perp(P_{2b}) = -30.85$
			$\tau_{\|\|}(P_{1a}) = \tau_{\|\|}(P_{1b}) = 202.1$	$\tau_{\|\|}(P_{2a}) = \tau_{\|\|}(P_{2b}) = 63.27$
$\mathbf{3''_b}^{\bullet-}$	$P_{1a} = P_{1b} = 41.27$	$P_{2a} = P_{2b} = 17.28$	$\tau_\perp(P_{1a}) = \tau_\perp(P_{1b}) = -102.0$	$\tau_\perp(P_{2a}) = \tau_\perp(P_{2b}) = -33.5$
			$\tau_\perp(P_{1a}) = \tau_\perp(P_{1b}) = -95.78$	$\tau_\perp(P_{2a}) = \tau_\perp(P_{2b}) = -32.0$
			$\tau_{\|\|}(P_{1a}) = \tau_{\|\|}(P_{1b}) = 197.86$	$\tau_{\|\|}(P_{2a}) = \tau_{\|\|}(P_{2b}) = 65.55$

Table 10. Calculated Geometrical Parameters (Å, deg) for the Singlet and Triplet States of $[\mathbf{3}]^{2-}$

params	singlet (planar)	triplet (planar)	singlet (not planar)	triplet (not planar)
$P_{1a}-P_{2a}$	2.156	2.155	2.150	2.154
$P_{2a}-C_1$	1.776	1.843	1.822	1.844
$C_{1a}-P_{1a}$	1.830	1.827	1.860	1.826
$C_{1a}-C_{6a}$	1.423	1.423	1.407	1.422
C_1-C_6	1.434	1.414	1.400	1.412
$P_{2a}-P_{1a}-C_{1a}$	102.42	102.78	99.5	102.72
$P_{1a}-P_{2a}-C_1$	105.86	103.36	103.77	102.93
$P_{1a}-P_{2a}-C_1-C_6 = \xi_1$	0.0	0.1	91.8	21.74
$C_{1a}-P_{1a}-P_{2a}-C_1$	180.0	180.0	179.9	174.3
$C_{2a}-C_{1a}-P_{1a}-P_{2a} = \xi_2$	0.0	0.0	0.38	4.0
rel energy (kcal mol^{-1})	0.0	2.4	21.3	2.3

Single-crystal X-ray structures of the singly reduced forms of **1**−**3** are currently unavailable, but reasonable structures can be inferred from combining the DFT and EPR results. First, it is necessary to confirm that the hyperfine couplings calculated for the model anions $\mathbf{1'}^{\bullet-}$, $\mathbf{2'}^{\bullet-}$, and $\mathbf{3'}^{\bullet-}$ are consistent with the values measured for $\mathbf{1}^{\bullet-}$, $\mathbf{2}^{\bullet-}$, and $\mathbf{3}^{\bullet-}$ respectively. The ^{31}P isotropic coupling constants calculated for the model anions are practically the same for the two planar isomers (**a** or **b**) and smaller than the values measured for the real anions. Despite being smaller, they are not in great disagreement, when one considers that it is well-known that Fermi contact with phosphorus is difficult to predict with accuracy for widely delocalized systems with strong contributions of inner shell polarizations.[28] It is worthwhile mentioning that, as previously reported,[29] an appreciable increase in the ^{31}P isotropic coupling constants can be obtained by using IGLO-III and TZVP basis sets; the corresponding results for $\mathbf{1b}^{\bullet-}$, $\mathbf{2b}^{\bullet-}$, and $\mathbf{3b}^{\bullet-}$ are given as Supporting Information. The triplet of triplet and the triplet signals observed on the liquid-phase EPR spectra of $\mathbf{3}^{\bullet-}$ and $\mathbf{1}^{\bullet-}$, respectively, agree with the DFT predictions on $\mathbf{3'}^{\bullet-}$ and $\mathbf{1'}^{\bullet-}$. Moreover, the anisotropic tensors measured for these two species are in satisfactory agreement with the calculated ones and confirm the preponderant p character of the phosphorus orbital containing the unpaired electron. The DFT results on $\mathbf{2'}^{\bullet-}$, however, suggest that the triplet signals observed with $\mathbf{2}^{\bullet-}$ results from hyperfine coupling with the

(28) (a) Nguyen, M. T.; Creve, S.; Eriksson, L. A.; Vanquickenborne, L. G. *Mol. Phys.* **1997**, *91*, 537. (b) Chentit, M.; Sidorenkova, H.; Choua, S.; Geoffroy, M.; Ellinger, Y.; Bernardinelli, G. *J. Organometallic. Chem.* **2001**, *634*, 136. (c) Cramer C. J.; Lim, M. H. *J. Phys. Chem.* **1994**, *98*, 5024.

(29) Nguyen, M. T.; Creve, S.; Vanquickenborne, L. G. *J. Phys. Chem. A* **1997**, *101*, 3174.

Chart 1

	X	Y	R'	R
1	P	CH	H	Mes
2	CH	P	*p*-$C_6H_4{}^tBu$	H
3	P	P	*p*-$C_6H_4{}^tBu$	Mes
1'	P	CH	H	H
2'	CH	P	H	H
3'	P	P	H	H

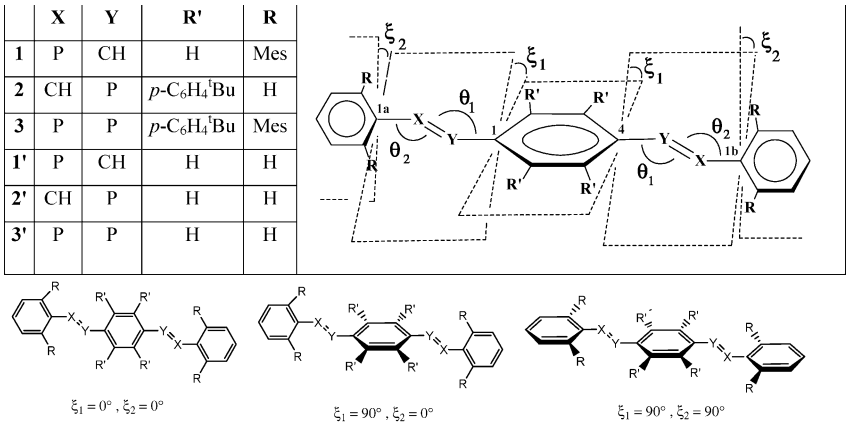

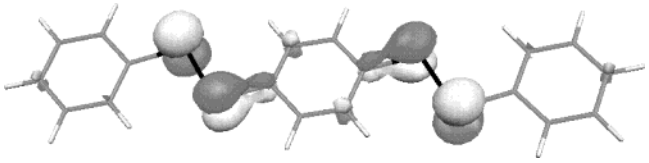

Figure 7. SOMO for $\mathbf{3}^{\bullet-}$ (planar geometry).

two phosphaalkenic protons. ^{31}P coupling, in this case, is probably not detected due to the poor resolution of the spectra. The absence of any resolved hyperfine splitting on the frozen solution spectrum confirms that, for $\mathbf{2}^{\bullet-}$, the phosphorus spin densities are indeed very small.

With the demonstration of a correlation between the DFT-calculated spin densities and the EPR data, the geometry of the radical anions can be addressed. In $\mathbf{1'}^{\bullet-}$, $\mathbf{2'}^{\bullet-}$, and $\mathbf{3'}^{\bullet-}$ the addition of an electron makes the molecule planar and causes an increase of the P═X or Y═P distance. This is in accord with the SOMOs, which, as seen in Figure 7 for $\mathbf{3}^{\bullet-}$, are antibonding between phosphorus and the X or Y atom but bonding between Y and C1 (or C4). They clearly show that the unpaired electron is strongly localized in a p_π orbital of each X atom, while the spin densities on the two Y atoms remains lower. These characteristics of the planar radical anions are readily seen from the calculated ^{31}P isotropic coupling constants: two large constants (∼50 MHz) and two medium (13 MHz) for $\mathbf{3'}^{\bullet-}$; two large constants (50 MHz) for $\mathbf{1'}^{\bullet-}$; two very small constants for $\mathbf{2'}^{\bullet-}$ (2 MHz).

To check to what extent the phosphorus hyperfine couplings are sensitive to a lack of planarity of the P═PC_6H_4P═P backbone in the radical monoanion, we have calculated these coupling constants for $\mathbf{3'}^{\bullet-}$ by assuming that the dihedral angles ($\xi_1 = 84°$, $\xi_2 = 46°$) obtained from the crystal structure of **3** were retained:[30] A_{iso}(P1a, P1b) = 30 MHz; A_{iso}(P2a, P2b) = 37 MHz. Similar calculations on $\mathbf{3''}^{\bullet-}$, for $\xi_1 = 60°$, lead to A_{iso}(P1a, P1b) = 38 MHz and A_{iso}(P2a, P2b) = 32 MHz. It is clear that when the two P═P bonds are not coplanar with the central aromatic ring, the difference between the coupling of the external and internal phosphorus nuclei drastically decreases and, furthermore, is not in agreement with experimental results. In addition, the fact that the ^{31}P coupling constants calculated for various conformations of $\mathbf{3'}^{\bullet-}$ are similar to the corresponding values calculated for $\mathbf{3''}^{\bullet-}$ indicates that these phosphorus couplings are not very sensitive to the ξ_2 dihedral angle. It is also important to note that, at variable temperatures, no dynamic process is detected that might suggest a facile exchange of the unpaired electron between the two diphosphene moieties on the EPR time scale. Moreover, in accord with a delocalization of the unpaired electron on the whole molecule, the frozen solution spectrum indicates that even at low temperature the hyperfine pattern results from a coupling with two pairs of ^{31}P nuclei. This spectrum is drastically different from that observed on the frozen solution spectrum of $\mathbf{4}^{\bullet-}$ which results from the coupling with two magnetically nonequivalent ^{31}P nuclei (Figure 6c). This result is consistent with the electrochemical data and the resultant large K_{com} value.

The EPR spectra described above are therefore in accord with minimally- planar X═Y−Ph−Y═X array for the three monoanions. Structures having all three aromatic rings in the line of potential conjugation coplanar are not tenable, however, owing to the massive sizes of the protecting groups. In fact, this conformation would be very remarkable for $\mathbf{3}^{\bullet-}$, whereas the crystal structure of the parent neutral molecule clearly indicates a nonplanar Ph−X═Y−Ph−Y═X−Ph array ($\xi_1 = 84°$; see above). In the structure of **3** ($\xi_2 = 46°$) and that of DmpP═PDmp, one of the aromatic residues tends to become coplanar with the two phosphorus atoms.

Noting the inaccessibility of a planar Ph−X═Y−Ph−Y═X−Ph array, the resonance structures that best represent the monoanions are shown as mesomeric forms **A** and **A′**. These two structures which require ξ_1 to be close to zero but, formally, accept any value for ξ_2, nicely fit the observed data, especially the spin densities on X. In reality, if ξ_1 be close to zero, then ξ_2 is most likely near 90° to minimize steric conflicts between bulky substituents. Careful analysis of Tables 4, 6, and 8 also reveals that the Y−C4 (and Y−C1) bond lengths decrease upon reduction (0.033, 0.035, and 0.034 Å for **1′**, **2′**, and **3′**, respectively); similarly the C2−C3 bond lengths decrease while the C1−C2 distances

(30) In these calculations performed on $\mathbf{3_b'}^{\bullet-}$ and $\mathbf{3_b''}^{\bullet-}$, the torsion angles ($\xi_1$ for $\mathbf{3_b'}^{\bullet-}$ and $\mathbf{3_b''}^{\bullet-}$ and ξ_2 for $\mathbf{3_b'}^{\bullet-}$) are fixed and the other parameters are allowed to relax.

increase. All the available data are consistent with the involvement of quinone-like resonance structures **A** and **A′**.

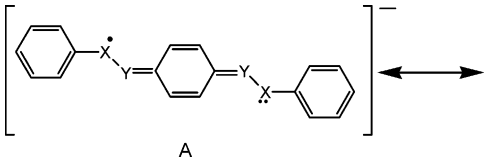

A

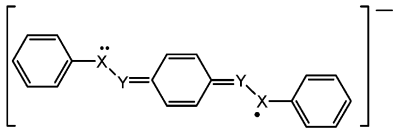

A'

Doubly Reduced Bis(diphosphene). Unlike the diphosphaalkenes, bis(diphosphene) **3** could be reduced to a relatively stable dianion using chemical reductants. This two-electron reduction product was EPR active, and as shown in Figure 4, its room temperature spectrum was quite different from that observed with the radical monoanion (Figure 3) since it simply consists as a doublet of doublets ($A_{iso}(^{31}P)$ = 173 MHz, $A_{iso}(^{31}P)$ = 78 MHz).

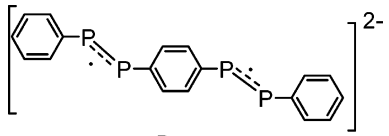

B

For a biradical $[\mathbf{3'}]^{2-}$, of the **B** type, containing two unpaired electrons delocalized on the planar system, the exchange parameter J is expected to be large and probably superior to the hyperfine couplings. This assumption is confirmed by the DFT results which show that the energy difference between the triplet and the singlet state is equal to 810 cm^{-1} whereas the experimental ^{31}P coupling[31] is less than 10^{-2} cm^{-1}. In this case, the ^{31}P hyperfine structure for $[\mathbf{3}]^{2-}$ should correspond to that produced by a molecule containing two equivalent diphosphene monoanions, with ^{31}P coupling constants equal to half the value measured for an isolated $(RP{=}PR')^{\bullet-}$ species. The coupling constants (A_1 = 204 MHz, A_2 = 95 MHz) reported in Table 3 for the asymmetric diphosphene anion Mes*P=PDmp (**4**) suggest therefore that a dianion $[\mathbf{3}]^{2-}$, which adopts the planar structure **B**, would lead to a triplet of triplets characterized by coupling constants of ca. 100 and ca. 45 MHz. Clearly this analysis is not consistent with the very simple experimental spectrum, moreover, since any mixing between the singlet and triplet state (which would occur if J became comparable to the hyperfine interaction) is expected to make the spectrum still more complex. The only reasonable interpretation for experimental EPR spectrum of $[\mathbf{3}]^{2-}$ is to assume that each diphosphene moiety bears an unpaired electron (occupying the P=P π^* orbital) and is independent of the other CPPC group (structure **C**). This assessment is consistent with the fact that the two ^{31}P isotropic coupling constants found for $[\mathbf{3}]^{2-}$ (173, 78 MHz) are rather close to those measured for the monomer $\mathbf{4}^{\bullet-}$ (204, 90 MHz). Structure **C** (Chart 2) illustrates how the middle ring adopts an orientation that "insulates" the spins from one another. Distortions from this idealized structure toward structure **B** will of course make spectral interpretation more difficult.

Chart 2

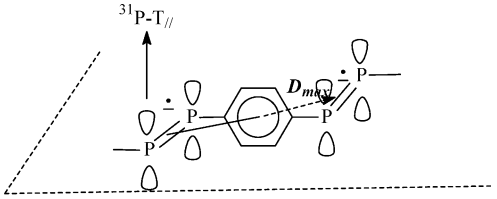

C

The frozen solution spectra are not in conflict with this interpretation. If the dipolar splitting with an extra proton observed on the frozen solution of $\mathbf{4}^{\bullet-}$ is disregarded, the spectrum obtained at 100 K with $[\mathbf{3}]^{2-}$ differs from that obtained with $\mathbf{4}^{\bullet-}$ only in its central part. This difference is probably due to the small dipolar electron−electron interaction tensor **D** between the two P=P moieties which is oriented perpendicular to the two ^{31}P hyperfine tensors (Chart 2). However, this dipolar interaction is rather small, in accord with the absence of any forbidden ($\Delta M_s = 2$) transition at half-field. All these spectral characteristics correspond to the limiting case $J = 0$ and again suggest a substructure for the dianion as portrayed by **C**.

Conclusion and Summary

The structures of **1**−**3** and their reduced products have been examined by a combination of crystallographic, EPR spectroscopic, and calculational methods. The following provides a recap:

Neutrals. Structural studies of the neutral molecules **2** and **3**, in conjunction with DFT studies of models **1′**−**3′**, suggest that steric interactions do not allow orientations which simultaneously place all three aromatic residues that directly attached to the P=X groups in **1**−**3** into a planar Ph−X=Y−Ph−Y=X−Ph array. At best, only one of the two aromatic residues across an X=Y unit can become coplanar at one time. Thus, for neutrals **1** and **2**, which have one large aromatic group and one small phenyl ring across each X=Y unit, the most probable structures have pairs of dihedral angles ξ_1 near 0°, ξ_2 near 90° and ξ_1 near 90°, ξ_2 near 0°. For **3**, while the solid state approximates **2**, the UV−visible spectrum shows a red shift of 18−20 nm for both the n ↔ π^* and the π ↔ π^* transitions relative to DmpP=PDmp (**5**)[23] and thus indicates that some conjugation occurs and perhaps some rotation about the P−C_{aryl} bonds to oscillate various values of ξ_1 and ξ_2, such that the sum of the two angles is close to 90°.

Monoanions. The calculational and EPR studies indicate that upon reduction **1**−**3** all adopt quinoidal-type structures

(31) A maximum value for the ^{31}P hyperfine structure can be estimated from the largest ^{31}P coupling measured for the nonsymmetrical diphosphene anion $\mathbf{4}^{\bullet-}$: A_{iso} = 196 MHz; $T_{||}$ = 516 MHz (0.017 cm^{-1}).

Chart 3

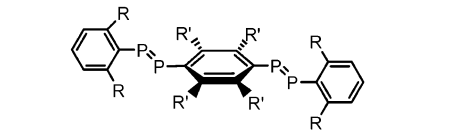

$\xi_1 = \sim 90°$, $\xi_2 = \sim 0°$

3

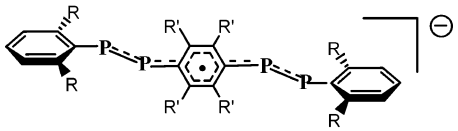

$\xi_1 = \sim 0°$, $\xi_2 = \sim 90°$

$\mathbf{3}^{\bullet-}$

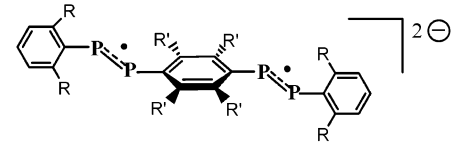

$\xi_1 = \sim 90°$, $\xi_2 = \sim 0°$

$\mathbf{3}^{2-}$

that dictate that the central phenylene ring is coplanar with the two attached X−Y units.

Dianion. Doubly reduced **3** is EPR active, and analysis of these data, in conjunction with the DFT results for model compounds, indicate that despite small electronic preferences for such a system to provide a maximally conjugated system and a (probably) diamagnetic molecule, steric interactions enforce a conformation that leads to the insulation of the two spins from one another and a paramagnetic system. This conformation is essentially a reversal to the locked conformation deduced for the monoanion of **1**−**3**; i.e., ξ_1 increases from 0 to 90°. The resulting geometrical changes upon successive reduction for **3** are illustrated in Chart 3.[32] The shuttling of ξ_1 and ξ_2 dihedral angles show how one might consider the redox-induced geometrical changes for **3** analogous to behavior of a so-called molecular switch. These results thus suggest that steric forces can play critical roles in the design of future materials for molecular electronics.

Acknowledgment. We thank the National Science Foundation (for J.D.P., Grant CHE-9733412) and the Swiss National Science Foundation (for M.G., Grant 2000-068179.02) for support of this research.

Supporting Information Available: A table of hyperfine coupling constants calculated with additional basis sets (IGLO-III, TZVP). This material is available free of charge via the Internet at http://pubs.acs.org.

IC030079J

(32) In contrast with ξ_1, the value of ξ_2 probably does not considerably affect the EPR spectra; the values of ξ_2 shown for $\mathbf{3}^{\bullet-}$ (90°) and $\mathbf{3}^{2-}$ (0°) are therefore compatible with the spectra but not required.